

# Reorganizing attention-space geometry with expressive attention

Claudius Gros

Institute for Theoretical Physics  
Goethe University Frankfurt  
Frankfurt a. M., Germany  
[{gros07}@itp.uni-frankfurt.de](mailto:{gros07}@itp.uni-frankfurt.de)

## Abstract

Attention involves comparing query and key vectors in terms of a scalar product,  $\mathbf{Q}^T \mathbf{K}$ , together with a subsequent softmax normalization. Classically, parallel/antiparallel queries and keys lead to large/small attention weights. Here we study expressive attention (EA), which is based on  $(\mathbf{Q}^T \mathbf{K})^2$ , the squared dot product. In this case attention is enhanced when query and key are either parallel or antiparallel, and suppressed for orthogonal configurations. EA can be introduced into any attention-based code without additional compute costs or memory requirements. For a series of autoregressive prediction tasks, we find that EA performs at least as well as the standard mechanism, dot-product attention (DPA). Increasing task complexity, EA is observed to outperform DPA with increasing margins, which also holds for multi-task settings. For a given model size, EA manages to achieve 100% performance for a range of complexity levels not accessible to DPA.

## Introduction

Since its inception (Bahdanau, Cho, and Bengio 2014; Vaswani et al. 2017), the attention mechanism has had a transformative impact on machine learning (Soydaner 2022; Minaee et al. 2024). At its core, attention facilitates pairwise information routing between tokens, with information being transmitted when a given matching condition is fulfilled. For the latter query and key vectors  $\mathbf{Q}$  and  $\mathbf{K}$  are compared in terms of the respective dot products,  $\mathbf{Q}^T \mathbf{K}$ , which are mapped to a normalized probability distribution via a subsequent softmax operation. As illustrated in Fig. 1, this setup, dot-product attention (DPA), constrains the central part of the matching condition to a one-dimensional subspace of the otherwise potentially large space of attention heads. Given that attention matrices tend to be sparse (Likhosherstov, Choromanski, and Weller 2023), it might be favorable to allow the system to express low attention states in a larger subspace.

Here we introduce and discuss a modified attention mechanism, expressive attention (EA), which is based on the presumption that low attention should correspond to orthogonal query and key configurations. This venue allows attention to express itself in the entire attention space, as illustrated in

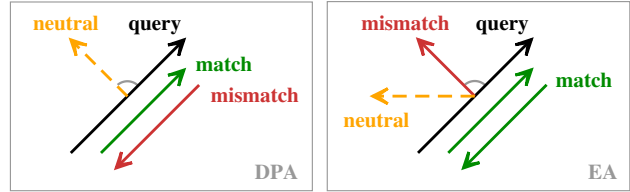


Figure 1: Comparing keys (colored arrows) with a given query (black arrow), constitutes the basis of ML attention. Attention weights are large/small when query and key match/mismatch (green/red), or in between, viz neutral (dashed yellow). For the standard dot-product attention (DPA, left panel, see (1)), attention weights are large/small for parallel/antiparallel keys and query. For expressive attention (EA, right panel, defined in (2)), both parallel and antiparallel alignments form matching pairs, with orthogonal keys and queries leading to a mismatch.

Fig. 1. All one needs to realize EA is to base attention on  $(\mathbf{Q}^T \mathbf{K})^2$ , the squared scalar product. In practice, this corresponds to changing a single line of code, which makes it straightforward to introduce effective attention into production codes. Computational complexity and memory requirements are not affected.

We present a comparative evaluation of classical DPA and EA. For this purpose we employ a suite of autoregressive prediction tasks (NT prediction tasks) that are based on time series generated by the delayed addition of two or more numbers, where addition is modulo a generic basis  $N$ , like 2 or 16 (binary/hexadecimal case). NT tasks are generalized delayed XOR tasks that become increasingly difficult to solve for larger  $N$  and delays  $\tau$  (Schubert and Gros 2021). Models are expected to achieve not just a good performance, but 100%, which reflects the view that systems can be said to exhibit reasoning errors when achieving less than 100% accuracy for solvable tasks (Liu et al. 2024). The question is then, how long perfect performance can be maintained when systematically increasing task difficulty, viz complexity.

## Related work

Alternatives to the standard, attention-based transformer have been studied intensively during the past years. At a ba-

sic level, non-transformer based architectures for sequence processing have been proposed, like structured and/or selective state sequence models (Gu, Goel, and Ré 2021; Gu and Dao 2023). Other approaches aim to reduce compute costs, for example by making use of a multi-to-multi recurrent network analogy (Feng et al. 2024). Another route is linearized attention (Katharopoulos et al. 2020; Wang et al. 2020; Wu et al. 2022) for which compute scales linearly with context length, and not quadratically. In practice, linear attention comes with various problems of its own, like unbounded gradients and attention dilution (Qin et al. 2022a; Han et al. 2023). In general, linearized attention models substitute the softmax operation of classical dot-product attention by various linear kernel functions, which may have stochastic components (Choromanski et al. 2020; Peng et al. 2021), well designed spatial dependencies (Qin et al. 2022b), or being derived from a singular value decomposition (Chen et al. 2024).

A different aspect is addressed by rotary positional embedding (RoPE), which adds positional information directly to the attention mechanism, via position-dependent rotations of query and key vectors (Su et al. 2021, 2024). RoPE can be used in particular for extending context windows (Chen et al. 2023). Somewhat similar in spirit is  $(IA)^3$ , which uses element-wise rescaled key and values vectors (in addition to rescaled hidden layer activities) for fine-tuning pretrained LLMs for downstream tasks (Liu et al. 2022).

Two main routes are available for testing the performance of sequence processing architectures, such as transformers. The first is to use databases relevant for real-world applications (Kaddour et al. 2023; Yang et al. 2024), the second is to rely on synthetic test suites. The latter approach is used standardly when studying learning biases, e.g., when comparing length generalization scores for functions like ‘parity’, ‘majority’, ‘first’ or ‘mean’ (Abbe et al. 2023; Hahn and Rofin 2024). Synthetic test environments have been employed also for the study of attention glitches in reasoning tasks (Liu et al. 2024). For our studies we use NT tasks, a suite of synthetic autoregressive prediction tasks which can be tuned to a desired level of difficulty, viz complexity. We will study in particular the transition between good and optimal performance when increasing context length.

## Background

Multiplying token activity with the respective query, key and value matrices generates three vectors,  $\mathbf{Q}_i$ ,  $\mathbf{K}_i$  and  $\mathbf{V}_i$ , specifically for each token  $i$  in a given attention layer. The activity  $y_m$  of token  $m$  is given by  $y_m = \sum_{k \leq m} a_{mk} \mathbf{V}_k$ , when masked attention is used. The attention matrix  $a_{mk} \geq 0$  is normalized row-wise,  $1 = \sum_k a_{mk}$ , encoding how much information is transferred from token  $k$  to token  $m$ . This setup implements information routing for any suitable mechanism determining the individual  $a_{mk}$ . The standard approach (Vaswani et al. 2017),

$$a_{mk} \Big|_{\text{DPA}} = \frac{1}{Z_m} \exp(\beta \mathbf{Q}_m^T \mathbf{K}_k) \quad (1)$$

takes the scalar product  $\mathbf{Q}^T \mathbf{K}$  as the fundamental similarity measure. The softmax operation included in (1) transforms

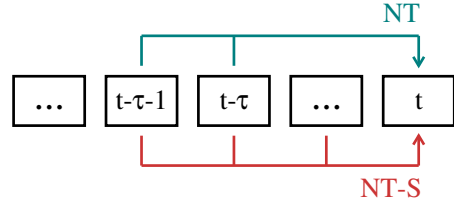


Figure 2: For a time series of symbols (boxes), the structure of the NT prediction task (teal), as defined by (4), and of the NT-S variant (red), see (8).

the basic similarity measure into a probability distribution function, with  $Z_m$  being an appropriate normalization factor. One can set  $\beta = 1$  without affecting performance, as done here, as the standard expression  $\beta = 1/\sqrt{N_{\text{con}}}$  only affects the scaling of weight and query matrices with context length,  $N_{\text{con}}$  (Vaswani et al. 2017).

As an alternative to (1) we investigate expressive attention (EA), defined by

$$a_{mk} \Big|_{\text{EA}} = \frac{1}{N_m} \frac{z_{mk}^2}{1 + z_{mk}^2}, \quad z_{mk} = \mathbf{Q}_m^T \mathbf{K}_k, \quad (2)$$

where  $N_m$  is a normalization factor. An illustration is presented in Fig. 1. Importantly, EA is a function of the squared dot-product  $z_{mk}$ . The difference between EA and DPA can be expressed in terms of attention space geometry.

**Attention space geometry** Attention mechanisms based on comparing keys and query vectors allocate semantic meanings to the respective geometric configurations. Classically (1), parallel/anti-parallel keys and queries lead to high-/low attention weights. For a  $d$ -dimensional attention-head space, the  $d - 1$  possible orthogonal arrangements lead to intermediate attention weights.

Full attention matrices tend to be sparse (Likhosherstov, Choromanski, and Weller 2023), which allows in many instances to reduce the dimensionality of attention matrices from the start via a dedicated decimation process (Roy et al. 2021; Lou et al. 2024). This observation suggest that it may be advantageous if all possible  $d - 1$  dimensional orthogonal configurations would lead to reduced attention weights. Eq. (2) encodes this concept, as illustrated in Fig. 1. The naming of our approach, ‘expressive attention’, is motivated by above geometric considerations.

## Experimental settings

**Suite of Tasks** A basic non-linear autoregressive task is to predict the next token of a time series (Li et al. 2024a). For our investigation we are interested in a suite of time series prediction tasks which allows to systematically increase and tune difficulty. As a motivation we first consider the basic XOR setting (Gros 2024).

$$\begin{aligned} x(t) &= \text{XOR}(x(t-1), x(t-2)) \\ &= [x(t-1) + x(t-2)] \% 2, \end{aligned} \quad (3)$$

where we used in the second step that the XOR operation correspond to the addition of two boolean inputs  $x = 0/1$ ,

modulo two. As illustrated in Fig. 2, we generalize (3) to the case of a general delay  $\tau \in [1, 2, 3, \dots]$  and basis  $N \in [2, 3, 4, \dots]$ ,

$$\text{NT: } x(t) = [x(t - \tau) + x(t - 1 - \tau)] \% N, \quad (4)$$

which defines the NT prediction task. For the XOR series, recovered for N2T1, two types of cyclic patterns are generated,

$$011011011011 \dots, \quad 000000000000 \dots \quad (5)$$

There are four initial conditions, 11, 01, 10 and 00, of which the first three give rise to cycles of type 011, with the last leading to the default series. The complexity of the associated prediction task increases systematically when increasing  $N$  and/or  $\tau$ . For example, one has

$$512 \cdot 120 + 64 \cdot 60 + 8 \cdot 30 + 1 \cdot 15 + 1 \cdot 1 = 65536 = 16^4 \quad (6)$$

for N16T3, which states that there are  $512/64/8/1/1$  cycles of length 120/60/30/15/1. One recovers the  $N^{\tau+1} = 16^4$  possible initial conditions when summing up all cycles together with their respective multiplicities. The most demanding system examined in this study is N16T5, for which  $16^6 = 2^{24} \approx 16.8 \text{ M}$  initial conditions exists, together with a corresponding number of distinct cycles.

**Transformer details** As a testbed, we use a decoder-only transformer architecture with position-specific encoding matrices, a variant denoted ‘cisformer’ (Gros 2025). We work with  $N_{\text{con}}$  context token and an embedding dimension  $d = N$ , where  $N$  is the basis of the NT task, see Eq. (4). A straightforward orthogonal token embedding of the  $N$  symbols  $\{0, 1, 2, \dots, N-1\}$  is implemented. Attention is causal. Expressive attention works perfectly with standard positional embedding schemes, which we did however not include. This simplifies the analysis of performance as a function of input length. A single transformer bilayer is used throughout this study, with one attention head per token. Skip connections are present, with layer normalization being performed on entry, separately for the attention and the token-wise, tanh feedforward layer. The width of the feed-forward hidden layer is expanded by a factor four.

**Training** Training is performed as a function of epochs, with each epoch consisting of  $N_{\text{batch}}$  predictions. At the start of each epoch a new random NT series is generated and encoded. The first  $N_{\text{con}}$  symbols are then loaded into context space. For the underlying sequence we define a batch as the task to predict one-by-one the next  $N_{\text{batch}} = 40$  symbols. A basic SGD optimizer is used during training, with momentum  $\mu = 0.8$  and a learning rate  $\epsilon = 0.02$ . Our aim is for a testbed that allows to study relative performance, in particular as a function of the complexity of the task, and not to attain optimal performance by fine-tuning meta parameters. If not stated otherwise, results shown are averaged over  $N_r = 16$  independent runs,

**Readout & Testing** The readout token is connected via a  $dN_{\text{con}} \times d$  matrix to the uppermost layer, with the task being to predict the next symbol of a NT time series. For the loss function the basic squared difference is taken, inference is

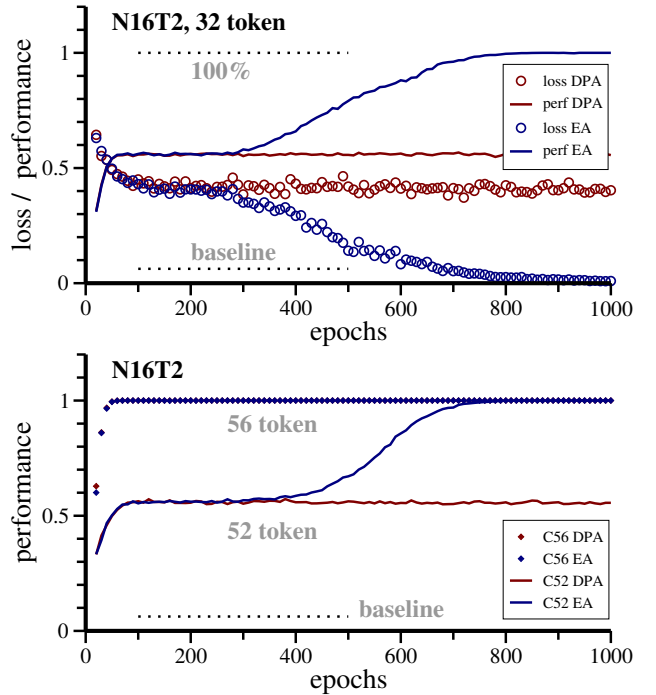


Figure 3: For a NT task with basis  $N = 16$  and delay  $\tau = 2$ , the performance (lines) and the loss (rescaled by a factor 0.75, circles). Result are for the standard dot-product attention (DPA, maroon), and for expressive attention (EA, blue). Performance is  $1/16 = 0.0625$  (baseline) when predictions are random, and 100% when no errors are made. Shown are results for a context length of 32 token (top panel) and 56 token (bottom panel), with DPA needing 56 token to achieve 100% performance. In this case, EA/DPA shown nearly identical training behavior.

greedy. During training, model performance is evaluated by asking the system to predict  $N_g = 50$  subsequent symbols of  $N_{\text{test}} = 100$  distinct, randomly generated NT series. Once training is finished, larger numbers of  $N_{\text{test}}$  are used for the final evaluation, at least  $N_{\text{test}} = 10^4$ . The aim is to achieve 100% accuracy.

**Learning strategies** For NT tasks, the symbols to be predicted are determined exclusively by two tokens situated at fixed positions from the right end of the input sequence. As a matter of principle, the complexity of the task would independent of  $N$ ,  $\tau$  and  $N_{\text{con}}$ , the context length, if the models tested would focus attention on exactly these two input positions. Our results indicate that this is not the case. Perfect performance is achieved nevertheless regularly, which implies that the respective strategies must be based on exploiting longer-range causal correlations. When using this class of strategies, task complexity does increase exponentially both with the size of the basis and the delay,  $N$  and  $\tau$ , becoming easier on the other hand when increasing context length.

## Results

A representative result is presented in Fig. 3, where simulations for  $N = 16$  and  $\tau = 2$  are shown for both types of attention, EA and DPA. This is a task of moderate complexity, with

$$64 \cdot 56 + 16 \cdot 28 + 4 \cdot 14 + 1 \cdot 7 + 1 \cdot 1 = 4096 = 16^3, \quad (7)$$

compare (6), which means that there are  $64/16/4/1/1$  periodic patterns of lengths  $56/28/14/7/1$ . Three context lengths are considered,  $N_{\text{con}} = 32/52/56$ .

- 100% performance

Eventually, both systems achieve 100% accuracy, predicting correctly 100 successive tokens for  $10^4$  random starting N16T2 sequences.

- structural traps

Lowering  $N_{\text{con}}$ , eventually both algorithms become trapped in a structural local minimum. This is particularly evident for  $N_{\text{con}} = 32$ , as shown in Fig. 3. Both attention mechanism rapidly improve their performance, reaching a plateau of about 55%, which is substantially above baseline. At this point the DPA loss function stops improving, with progress slowing down for EA. The phenomenology seen indicates that the enhanced expressivity of EA allows the system to escape the local trap via a comparatively narrow escape route.

- apparent emergence

As a function of system size, the DPA performance rapidly increases from about 55% to 100%. This happens between  $N_{\text{con}} = 52$  and 56, but it would be wrong to interpret this performance jump as an ‘emergence phenomenon’. In fact, what happens is that the structural local trap disappears eventually when enlarging training space successively, an expected behavior.

- task complexity

For  $\tau = 2$ , only  $16^3 = 4096$  distinct sequences exists for  $N = 16$ . The task is hence of modest complexity, given that during training  $N_{\text{batch}} = 40$  shifted sequences are seen for any single epoch. It is hence not surprising that the problem can be solved within 100 epochs for both models when the context length is large enough. When reducing the number adjustable parameters, both models require however larger training compute, when not failing completely. E.g., for  $N_{\text{con}} = 16$  (not included in Fig. 3), expressive attention still converges to 100% performance, needing however about 2000 epochs.

The results presented in Fig. 3 show in addition that training performance is nearly identical for both attention mechanisms when the problem at hand can be solved easily with available resources.

**Binary sequences** It has been pointed out that an important aspect for our understanding of transformers is the study of their loss landscape (Hahn and Rofin 2024; Choromanska et al. 2015). In this context we further investigate the structural local minima observed in Fig. 3 by comparing the two attention mechanisms for the smallest possible embedding dimension,  $d = N$ , which is realized for the binary case

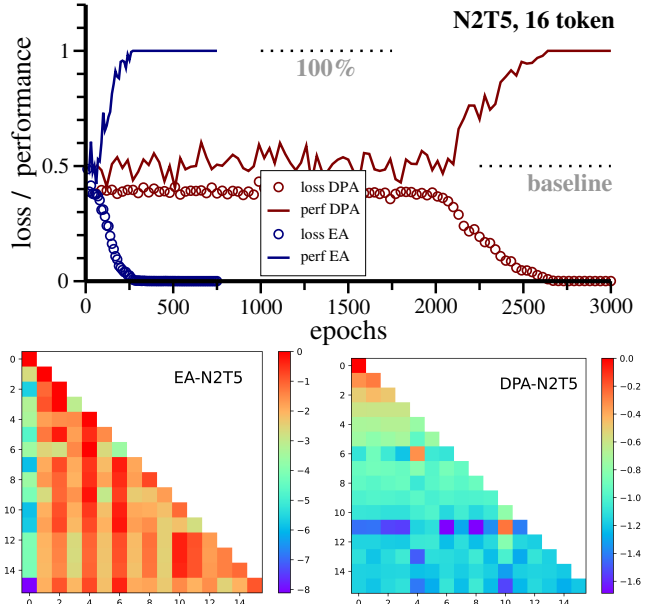


Figure 4: Results for a NT task with a binary basis,  $N = 2$ , and delay  $\tau = 5$ . The model contains 802 adjustable parameters for a context length  $N_{\text{con}} = 16$ , as used. **Top:** Loss (rescaled by 0.75) and performance. For otherwise identical parameters, dot-product attention (DPA) needs substantially longer to converge than expressive attention (EA). **Bottom:** Snapshots of the respective attention matrices. Typically, EA (left) covers a larger dynamical range (color-coding in  $\log_{10}$  scale), than DPA (right).

$N = 2$ , compare (4). An additional question is here whether EA is advantageous even in this limit.

We specialize to  $\tau = 5$ , for which there are just two NT sequences, namely the default state ‘00000’, and a cycle of length 63. Together the  $63 + 1 = 64 = 2^6$  possible initial conditions are covered, which makes N2T5 a seeming trivial task. For  $N_{\text{con}} = 16$ , and an embedding dimension  $d = N = 2$ , overall model size is however modest,  $N_{\text{model}} = 802$ , which may induce pronounced local minima in the loss landscape. This is indeed the case, as the results presented in Fig. 4 show. Averages over 16 runs have been taken.

For DPA one observes extended training spans during which performance fluctuates around the baseline, 50%, essentially without improving. For EA, the equivalent training stage is substantially shorter. The phenomenology observed indicates that learning is dominated by a stochastic escape process (Gros 2024). Stochastic escape is present when the additive effect of random fluctuating events allows systems to escape a local loss minimum. However, further studies would be needed to substantiate this hypothesis. Of relevance for our studies here is the observations that expressive attention may lead to a substantially faster convergence than the classical dot-product mechanism.

Also included in Fig. 4 are sample snapshots of the respective attention matrices. Visual inspection indicates that both models make use of the entire input sequence, viz that

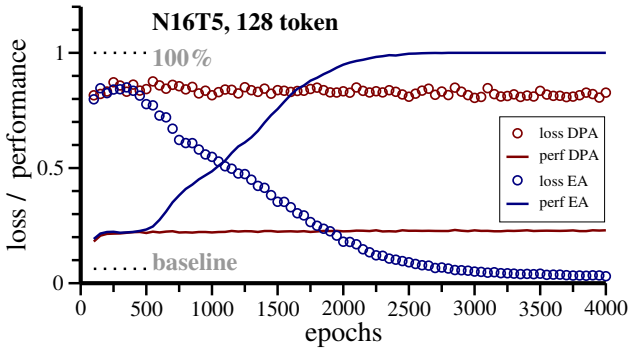


Figure 5: For a NT task with basis  $N = 16$ , delay  $\tau = 5$ , and 128 token, the performance (lines) and the loss (rescaled by a factor 0.75, circles). Qualitatively, the results mirror the ones presented in Fig. 3, both for the standard dot-product attention (DPA, maroon), and for expressive attention (EA, blue). When training for 2000 epochs, models see about  $0.5\% \text{ of } 16.8 \cdot 10^6$  possible sequences.

attention is not focused predominantly on the two causal token, as defined by (4).

**Large sequence spaces** The number  $N_{\text{seq}} = N^{\tau+1}$  of distinct NT sequences has been modest for the results presented in Figs. 3 and 4. As a consequence, exact solutions in the form of learned one-by-one mappings  $N_{\text{seq}} \rightarrow N$  are conceivable, at least as a matter of principle. This is however not any more the case for large  $N_{\text{seq}}$ .

In Fig. 5 we present results for N16T5. Model size is about  $4 \cdot 10^5$  for  $N_{\text{con}} = 128$ , in terms of adjustable parameters, which is substantially smaller than the number of distinct NT sequences,  $N_{\text{seq}} = 16^6 \approx 16.8 \cdot 10^6$ . During training,  $N_{\text{train}} = 0.8 \cdot 10^5$  training sequences are presented within the first 2000 epochs, which is about 0.5% of  $N_{\text{seq}}$ . It is hence likely that the generative mechanism has been encoded in one form or another once performance is either perfect, or near to 100%. As before, we used  $5 \cdot 10^5$  predictions for the evaluation.

On a qualitative level, the results shown in Figs. 5 and 3 are equivalent. Both attention mechanisms converge rapidly to a heuristic strategy with a non-trivial performance, respectively of the order of 0.55 for N16T2 and 0.2 for N16T5. In both cases, DPA remains stuck in the corresponding local minimum, with EA escaping at a reduced pace.

We did not determine at which context length DPA would converge. For  $N_{\text{con}} = 256$ , DPA remains in a local trap, but with an improved performance, of roughly 0.44. Increasing the context length further, to  $N_{\text{con}} = 512$ , we find that the training of both DPA and EA becomes unstable when our standard learning parameters are used, namely  $\mu = 0.8$  and  $\epsilon = 0.02$ . One could stabilize training by adjusting momentum and learning rate, which is however outside the scope of our comparative analysis.

**Mixture of tasks** The results presented till now concerned setups containing only a specific single tasks. We performed simulations also for mixture of tasks, finding that expressive

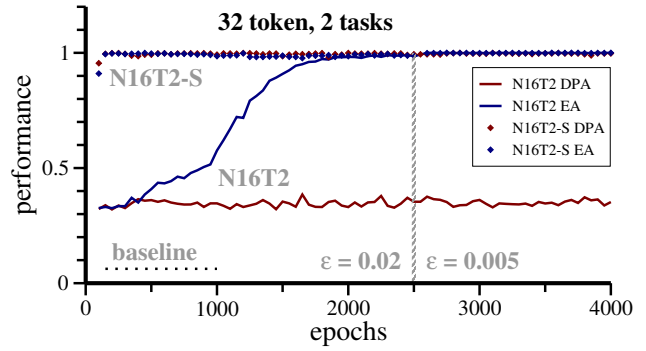


Figure 6: For a mixture of two tasks, N16T2 and N16T2-S, the performance of EA (blue) and DPA (maroon). Compare Fig. 3 for the case when only N16T2 is trained. After 2500 epochs (shaded vertical line), learning speed is reduced by a factor four.

attention outperforms classical dot-product attention generically also in this case. We define a new task variant, NT-S,

$$\text{NT-S: } x(t) = \left( \sum_{\Delta T=1}^{\tau+1} x(t - \Delta t) \right) \% N, \quad (8)$$

which corresponds to summing up the  $\tau+1$  preceding token, modulo  $N$ . The two versions, NT-S and NT are identical for  $\tau = 1$ , compare (4) and Fig. 2, but not for  $\tau > 1$ .

Results for  $N_{\text{con}} = 32$  are given in Fig. 6. During training a 50/50 mixture of N16T2 and N16T2-S autoregressive prediction tasks are presented as such, viz without further information. For a given prompt, which could be either a N16T2 or N16T2-S sequence, the system needs to determine on its own both the delay  $\tau$  and the type of the task at hand.

NT-S tasks typically lead to shorter cyclic patterns than the corresponding NT task, which makes them easier to learn. For example, the mean cycle length is 47.6 for N16T2, but only 23.8 for N16T2-S. Both systems, EA and DPA have consequently no problem to achieve 100% accuracy on N16T2-S as a single tasks. When combined with N16T2, both systems achieve still above 99% accuracy, as shown in Fig. 6. Also of interest is the reduction of the steady-state N16T2 performance in the mixed-task scenario, from about 0.55 to 0.34, which is also the value achieved by DPA.

In our setup, expressive attention is able to solve both tasks to about 99%. Given that N16T2 is shown only 50% of the time, it is not surprising that learning is prolonged, as evident from Fig. 6. As an experiment we lowered learning rate after 2500 epochs, finding that N16T2 performance increases a bit, by about 0.5%. Interference between competing tasks is reduced at lower learning rates.

Tasks are acquired consecutively in order of difficulty, as shown in Fig. 6, which can be interpreted as an instances of unsupervised curriculum learning (Bengio et al. 2009). Our results can be seen also as an explicit example of successive learning of task quanta, as postulated in the quantization theory of neural scaling (Michaud et al. 2024; Neumann and Gros 2022, 2024).

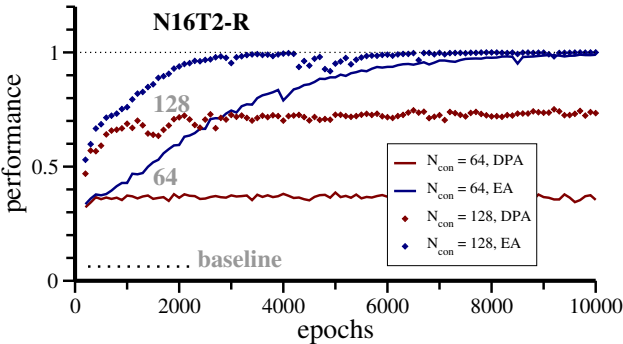


Figure 7: A N16T2 task switching conditionally to N16T2-S, as defined by (9). Data as averaged over 16 runs.

**Rare events** As a third variant, we introduce via

$$\text{NT-R: } \begin{cases} \text{NT-S} & \text{if } x(t-\tau-1) = 0 \\ \text{NT} & \text{otherwise} \end{cases} \quad (9)$$

a logical if-statement. The generating algorithm remains deterministic, switching from NT to NT-S when a given condition is fulfilled, here when  $x(t-\tau-1) = 0$ . For an observer this corresponds to a rare event that occurs with a probability of  $1/16=0.0625$  when  $N=16$ .

Determining the presence of an isolated hidden logical statement, as defined by (9), can be an exceedingly demanding task. In Fig. 7 results for  $N_{\text{con}} = 64/128$  are presented. For these two context lengths N16T2 is comparatively easy, as shown in Fig. 3, which implies that a certain level of performance should be attainable in any case. For DPA this level about 0.36 for  $N_{\text{con}} = 64$ , doubling to 0.72 when the context length is raised to 128.

The data presented in Fig. 7 demonstrate that it is difficult also for expressive attention to isolate a lone if-statement, as defined by (9). Training progress is slow, achieving in the end however an average accuracy of 98.8/99.9%, respectively for  $N_{\text{con}} = 64/128$ . As usual, averages over 16 random initial conditions have been taken. The majority of runs achieves however perfect performance. We did not investigate the cause of the non-monotonic events showing up during training, which may be due to periods with an increased clustering of rare events.

## Discussion

Obtaining encouraging results, we presented a first evaluation of expressive attention (EA), focusing on single-layer models with a single attention head. We also investigate models with two or more layers and/or attention heads, together with different learning speeds and/or momentum. All results are found to be robust. Additional investigation would however necessary for a full assessment of the potential of EA, e.g. in the realm of natural language processing (Kaddour et al. 2023; Yang et al. 2024), or within the context of formal languages (Strobl et al. 2024; Abbe, Adsera, and Misiakiewicz 2023). Generally, we expect that expressive attention will fare at least as well as dot-product attention (DPA), a presumption that is based on the respective design

principles. For DPA, large and small attention weights are constrained to a one-dimensional manifold within the space of attention heads, which is not the case for EA. The size of the performance boost obtainable when substituting DPA by EA may depend however strongly on the use case.

**Heuristics** Repeatedly we observed that initial performance gains flatten out rapidly. This happens in particular for small model sizes, but also for DPA in cases when the available resources are sufficient for EA to solve the problem at hand exactly. We argued that the resulting stationary performance plateau indicates the presence of a local minimum in loss landscape. From this trap models may escape either by an embedding into a larger dimensional parameter space, or by an improved design. For all cases the level of the observed stationary performance plateau was independent of initial conditions and training details. This led us to the conclusion that the associated local minimum in loss landscape is structural, viz that it corresponds to a heuristic strategy. To examine how this heuristic strategy works would an interesting research question, which is however beyond the scope of the present study.

**Reasoning** Inductive reasoning is one of the big challenges of large language models (Li et al. 2024b; Su et al. 2023). It is encouraging that one of the building blocks, the logical if-statement included, can be extracted and encoded when effective attention is used. Our analysis, which involved logical task switching within the NT-R framework (9), is however only a first indication and it remains to be seen to which extent EA may raise performance in this field.

**Acknowledgments** We thank Michael Hahn for discussions.

## References

Abbe, E.; Adsera, E. B.; and Misiakiewicz, T. 2023. Sgd learning on neural networks: leap complexity and saddle-to-saddle dynamics. In *The Thirty Sixth Annual Conference on Learning Theory*, 2552–2623. PMLR.

Abbe, E.; Bengio, S.; Lotfi, A.; and Rizk, K. 2023. Generalization on the unseen, logic reasoning and degree curriculum. In *International Conference on Machine Learning*, 31–60. PMLR.

Bahdanau, D.; Cho, K.; and Bengio, Y. 2014. Neural machine translation by jointly learning to align and translate. *arXiv preprint arXiv:1409.0473*.

Bengio, Y.; Louradour, J.; Collobert, R.; and Weston, J. 2009. Curriculum learning. In *Proceedings of the 26th annual international conference on machine learning*, 41–48.

Chen, S.; Wong, S.; Chen, L.; and Tian, Y. 2023. Extending context window of large language models via positional interpolation. *arXiv preprint arXiv:2306.15595*.

Chen, Y.; Tao, Q.; Tonin, F.; and Suykens, J. 2024. Primal-attention: Self-attention through asymmetric kernel svd in primal representation. *Advances in Neural Information Processing Systems*, 36.

Choromanska, A.; Henaff, M.; Mathieu, M.; Arous, G. B.; and LeCun, Y. 2015. The loss surfaces of multilayer networks. In *Artificial intelligence and statistics*, 192–204. PMLR.

Choromanski, K.; Likhosherstov, V.; Dohan, D.; Song, X.; Gane, A.; Sarlos, T.; Hawkins, P.; Davis, J.; Mohiuddin, A.; Kaiser, L.; et al. 2020. Rethinking attention with performers. *arXiv preprint arXiv:2009.14794*.

Feng, L.; Tung, F.; Hajimirsadeghi, H.; Ahmed, M. O.; Bengio, Y.; and Mori, G. 2024. Attention as an RNN. *arXiv preprint arXiv:2405.13956*.

Gros, C. 2024. *Complex and Adaptive Dynamical Systems: A Comprehensive Introduction*. Springer Nature.

Gros, C. 2025. Small transformer architectures for task switching. In *ICANN 2025*.

Gu, A.; and Dao, T. 2023. Mamba: Linear-time sequence modeling with selective state spaces. *arXiv preprint arXiv:2312.00752*.

Gu, A.; Goel, K.; and Ré, C. 2021. Efficiently modeling long sequences with structured state spaces. *arXiv preprint arXiv:2111.00396*.

Hahn, M.; and Rofin, M. 2024. Why are Sensitive Functions Hard for Transformers? *arXiv preprint arXiv:2402.09963*.

Han, D.; Pan, X.; Han, Y.; Song, S.; and Huang, G. 2023. Flatten transformer: Vision transformer using focused linear attention. In *Proceedings of the IEEE/CVF international conference on computer vision*, 5961–5971.

Kaddour, J.; Harris, J.; Mozes, M.; Bradley, H.; Raileanu, R.; and McHardy, R. 2023. Challenges and applications of large language models. *arXiv preprint arXiv:2307.10169*.

Katharopoulos, A.; Vyas, A.; Pappas, N.; and Fleuret, F. 2020. Transformers are rnns: Fast autoregressive transformers with linear attention. In *International conference on machine learning*, 5156–5165. PMLR.

Li, Y.; Huang, Y.; Ildiz, M. E.; Rawat, A. S.; and Oymak, S. 2024a. Mechanics of next token prediction with self-attention. In *International Conference on Artificial Intelligence and Statistics*, 685–693. PMLR.

Li, Z.; Cao, Y.; Xu, X.; Jiang, J.; Liu, X.; Teo, Y. S.; Lin, S.-w.; and Liu, Y. 2024b. LLMs for Relational Reasoning: How Far are We? *arXiv preprint arXiv:2401.09042*.

Likhosherstov, V.; Choromanski, K.; and Weller, A. 2023. On the expressive flexibility of self-attention matrices. In *Proceedings of the AAAI Conference on Artificial Intelligence*, volume 37, 8773–8781.

Liu, B.; Ash, J.; Goel, S.; Krishnamurthy, A.; and Zhang, C. 2024. Exposing attention glitches with flip-flop language modeling. *Advances in Neural Information Processing Systems*, 36.

Liu, H.; Tam, D.; Muqeeth, M.; Mohta, J.; Huang, T.; Bansal, M.; and Raffel, C. A. 2022. Few-shot parameter-efficient fine-tuning is better and cheaper than in-context learning. *Advances in Neural Information Processing Systems*, 35: 1950–1965.

Lou, C.; Jia, Z.; Zheng, Z.; and Tu, K. 2024. Sparser is Faster and Less is More: Efficient Sparse Attention for Long-Range Transformers. *arXiv preprint arXiv:2406.16747*.

Michaud, E.; Liu, Z.; Girit, U.; and Tegmark, M. 2024. The quantization model of neural scaling. *Advances in Neural Information Processing Systems*, 36.

Minaee, S.; Mikolov, T.; Nikzad, N.; Chenaghlu, M.; Socher, R.; Amatriain, X.; and Gao, J. 2024. Large language models: A survey. *arXiv preprint arXiv:2402.06196*.

Neumann, O.; and Gros, C. 2022. Scaling Laws for a Multi-Agent Reinforcement Learning Model. In *Deep Reinforcement Learning Workshop NeurIPS 2022*.

Neumann, O.; and Gros, C. 2024. AlphaZero Neural Scaling and Zipf’s Law: a Tale of Board Games and Power Laws. *arXiv preprint arXiv:2412.11979*.

Peng, H.; Pappas, N.; Yogatama, D.; Schwartz, R.; Smith, N. A.; and Kong, L. 2021. Random feature attention. *arXiv preprint arXiv:2103.02143*.

Qin, Z.; Han, X.; Sun, W.; Li, D.; Kong, L.; Barnes, N.; and Zhong, Y. 2022a. The devil in linear transformer. *arXiv preprint arXiv:2210.10340*.

Qin, Z.; Sun, W.; Deng, H.; Li, D.; Wei, Y.; Lv, B.; Yan, J.; Kong, L.; and Zhong, Y. 2022b. cosformer: Rethinking softmax in attention. *arXiv preprint arXiv:2202.08791*.

Roy, A.; Saffar, M.; Vaswani, A.; and Grangier, D. 2021. Efficient content-based sparse attention with routing transformers. *Transactions of the Association for Computational Linguistics*, 9: 53–68.

Schubert, F.; and Gros, C. 2021. Local homeostatic regulation of the spectral radius of echo-state networks. *Frontiers in computational neuroscience*, 15: 587721.

Soydaner, D. 2022. Attention mechanism in neural networks: where it comes and where it goes. *Neural Computing and Applications*, 34(16): 13371–13385.

Strobl, L.; Merrill, W.; Weiss, G.; Chiang, D.; and Angluin, D. 2024. What formal languages can transformers express? a survey. *Transactions of the Association for Computational Linguistics*, 12: 543–561.

Su, J.; Ahmed, M.; Lu, Y.; Pan, S.; Bo, W.; and Liu, Y. 2024. Roformer: Enhanced transformer with rotary position embedding. *Neurocomputing*, 568: 127063.

Su, J.; Lu, Y.; Pan, S.; Murtadha, A.; Wen, B.; and Liu, Y. 2021. RoFormer: Enhanced Transformer with Rotary Position Embedding. *arXiv preprint arXiv:2104.09864*.

Su, Y.; Fu, X.; Liu, M.; and Guo, Z. 2023. Are LLMs Rigorous Logical Reasoner? Empowering Natural Language Proof Generation with Contrastive Stepwise Decoding. *arXiv preprint arXiv:2311.06736*.

Vaswani, A.; Shazeer, N.; Parmar, N.; Uszkoreit, J.; Jones, L.; Gomez, A. N.; Kaiser, L.; and Polosukhin, I. 2017. Attention is all you need. *Advances in neural information processing systems*, 30.

Wang, S.; Li, B. Z.; Khabsa, M.; Fang, H.; and Ma, H. 2020. Linformer: Self-attention with linear complexity. *arXiv preprint arXiv:2006.04768*.

Wu, H.; Wu, J.; Xu, J.; Wang, J.; and Long, M. 2022. Flowformer: Linearizing transformers with conservation flows. *arXiv preprint arXiv:2202.06258*.

Yang, J.; Jin, H.; Tang, R.; Han, X.; Feng, Q.; Jiang, H.; Zhong, S.; Yin, B.; and Hu, X. 2024. Harnessing the power of llms in practice: A survey on chatgpt and beyond. *ACM Transactions on Knowledge Discovery from Data*, 18(6): 1–32.